

## Phasor analysis of atom diffraction from a rotated material grating

Alexander D. Cronin and John D. Perreault  
 University of Arizona, Tucson, Arizona 05721, USA

(Received 11 December 2003; revised manuscript received 15 June 2004; published 7 October 2004)

An atom-surface interaction was detected by studying atom diffraction from a rotated material grating. A phasor diagram similar to the Cornu spiral was developed to explain why there are no missing orders in atom diffraction from material gratings. We also show that atom-surface interactions combined with rotated grating structures can produce asymmetric, i.e., blazed, diffraction patterns. Our conceptual discussion is supported by experimental observations with a sodium atom beam and silicon nitride gratings. The data are consistent with the nonretarded van der Waals interaction.

DOI: 10.1103/PhysRevA.70.043607

PACS number(s): 03.75.Be

Atom diffraction from a material grating has recently been used to measure the strength of van der Waals interactions between atoms and the grating. This was possible in [1–3] because atom-surface interactions modify the intensity in each diffraction order as a function of atomic *velocity*. In this paper we measure van der Waals interactions by studying diffraction as a function of incidence *angle*. We also demonstrate an asymmetric atom diffraction pattern from a fabricated material grating.

Historically, a graphical analysis in the complex plane has been useful to understand optical diffraction. This is especially true for the Fresnel integrals for which no closed form analytical solutions have been found, yet the Cornu spiral permits a physical interpretation [4]. We have adapted this approach to our current problem in atom optics. Even in the far-field limit, van der Waals interactions modify atom diffraction such that no closed form analytical description has been found. Hence we developed a phasor diagram similar to the Cornu spiral to interpret our atom diffraction data.

In particular, we prove that no combination of grating geometry and van der Waals interaction strength can cause diffraction orders to disappear. This is proved using a phasor diagram, and confirmed experimentally by rotating a diffraction grating about an axis parallel to the grating bars while measuring the flux in each diffraction order.

In the standard theory of diffraction from a Ronchi-ruling, i.e., a square-wave absorbing grating, a missing order is obtained when

$$n = \pm \frac{m}{\eta}, \quad (1)$$

where  $n$  is the diffraction order,  $m$  is an integer greater than zero, and  $\eta$  is the open fraction defined as window size divided by grating period. For example, a 50% open fraction suppresses all the even orders.

The origin of missing orders in the diffraction theory can be explained with a phasor plot often referred to as a vibration curve [4,5]. In this approach a diagram in the complex plane [Fig. 1(a)] is used to visualize the amplitude and phase of the field in each diffraction order. In the Fraunhofer approximation, the field  $\Psi_n$  associated with the  $n^{\text{th}}$  diffraction order from a periodic array of apertures is

$$\Psi_n = \frac{\Psi_{inc}}{d} \int_{-w/2}^{w/2} e^{in\kappa\xi} d\xi, \quad (2)$$

where  $\Psi_{inc}$  is the incident wave amplitude,  $d$  is the grating period,  $w$  is the aperture width,  $\kappa = 2\pi(d)^{-1}$  is the grating wave number, and  $\xi$  is the spatial coordinate in the aperture along the grating wave vector.

This integral can be visualized by adding phasors of length  $d\xi$  and phase  $n\kappa\xi$  in the complex plane. Parametric curves generated this way are the real vs imaginary parts of the cumulative integral [Eq. (2)] for  $\Psi_n$ . The magnitude and phase of a resultant vector (from start to end of each cumulative integral) correspond to the complex amplitudes  $\Psi_n$  shown in Fig. 1(a). A resultant of zero magnitude represents a missing order.

Before including phase shifts due to atom-surface interactions, this integral can be computed analytically:

$$\Psi_n = \Psi_{inc} \eta \text{sinc}(n\eta), \quad (3)$$

where  $\text{sinc}(x) \equiv \sin(\pi x)/\pi x$ . For comparison with experiment, intensity is given by  $I_n = |\Psi_n|^2$ .

In the WKB approximation, to leading order in  $V(\xi)$ , van der Waals interactions cause a phase shift  $\phi_{vdw}(\xi)$  given by

$$\phi_{vdw}(\xi) = \frac{-V(\xi)l}{v\hbar}, \quad (4)$$

where  $V(\xi)$  is the van der Waals potential for atoms interacting with a surface,  $l$  is the distance the atom propagates in the potential,  $v$  is the atomic velocity, and  $\hbar$  is Planck's constant divided by  $2\pi$ . Near a surface (i.e.,  $r \ll \lambda_p$ ) the potential is known to be

$$V(r) = \frac{-C_3}{r^3}, \quad (5)$$

where  $r$  is the atom-surface distance and  $\lambda_p$  is the principle atomic transition wavelength [6]. For simplicity, as in [1–3],  $V(r)$  is approximated by Eq. (5) inside a grating window-slot of depth  $l$ , and approximated by zero outside the grating window.

van der Waals interactions with the bars on either side of the slot thus modify the phase of each point on the phasor diagram as shown in Fig. 1(b). This phase is described by

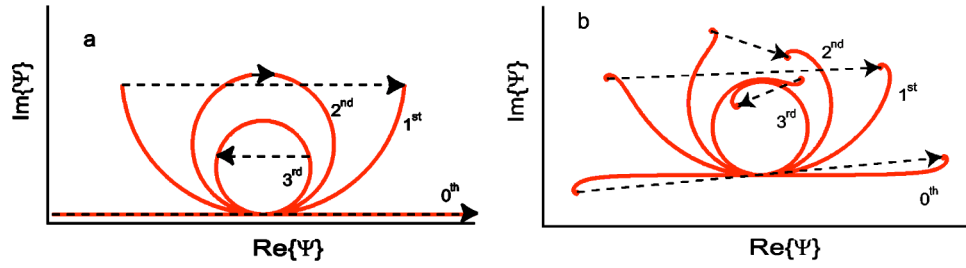


FIG. 1. (a) Phasor diagrams for diffraction into orders  $n=0,1,2,3$  from a grating with open fraction  $\eta=0.48$ . Resultant vectors are drawn with dashed lines from tip to tail of each curve. (b) van der Waals interactions modify the phasor diagram, and considerably increase the magnitude of the second order.

$$\Phi_n(\xi) = \phi_n(\xi) + \phi_{vdW}(\xi) + \phi_{offset}, \quad (6)$$

where  $\phi_n(\xi)$  is due to diffraction without an atom-surface interaction,  $\phi_{vdW}(\xi)$  is due to van der Waals interactions with surfaces located at  $\xi = \pm w/2$ , and a constant  $\phi_{offset}$  is added for reasons that will be discussed:

$$\phi_n(\xi) = n\kappa\xi, \quad (7)$$

$$\phi_{vdW}(\xi) = \frac{C_3 l}{v\hbar} [|\xi - w/2|^{-3} + |\xi + w/2|^{-3}], \quad (8)$$

$$\phi_{offset} = -\frac{16C_3 l}{v\hbar w^3}. \quad (9)$$

Examples of phasor diagrams for each diffraction order  $n = [0, 3]$  modified by  $\phi_{vdW}$  are shown in Fig. 1(b). Figure 2 shows several phasor diagrams for  $n=2$  given different values of  $C_3$ .

The constant  $\phi_{offset}$  is not physical but is chosen to be  $\phi_{offset} = -\phi_{vdW}(0)$  as a convenience. This permits comparison between shapes of the phasor diagrams for arbitrary  $C_3$ . This phase offset does not change the norm of the resultant amplitudes, hence it will not affect the argument regarding missing orders. It simply rotates the spirals in Fig. 2 to maintain the condition that  $\Phi_n(0) = 0$  independent of  $C_3$ . Thus, the tangent to each curve parallels the real axis when  $\xi = 0$ .

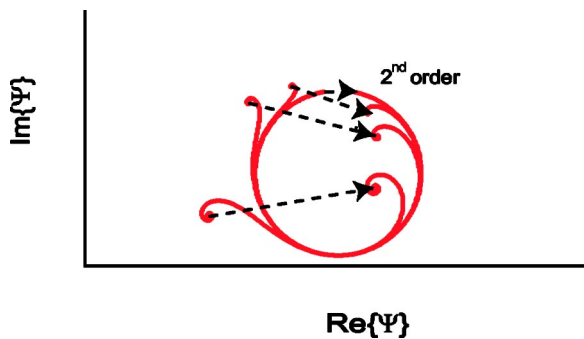


FIG. 2. Phasor diagrams for diffraction from a grating with open fraction  $\eta=0.48$  shown for diffraction order  $n=2$  given different values of the van der Waals coefficient  $C_3=0,1,10,100 \text{ eV \AA}^3$ . The resultant vectors from tip to tail are drawn with dashed lines.

For  $C_3=0$  the phasor curves lay on circles because the curvature, given by the derivative of phase with respect to  $\xi$ , is constant  $[(d/d\xi)\phi_n = n\kappa]$ . The phase difference between the endpoints of the curve [given by  $\phi_n(\xi=w/2) - \phi_n(\xi=-w/2)$ ] corresponds to the angle  $\kappa n w$ , and the arc length of the curve is given by the window size  $w$ . Thus the radius of the circle is  $\rho = (n\kappa)^{-1}$  and it is centered at the location  $i\rho$ . When the curve is an integral number of full circles, the endpoints overlap and the resultant field has zero magnitude. This corresponds to a missing order.

Additional phase due to van der Waals interactions makes the phasor curve deviate from a circle. One end of the spiral will always be *inside* the circle defined by  $\rho$  and the other end must be *outside*. This is true because the curvature  $[(d/d\xi)\Phi_n]$  increases monotonically as  $\xi$  increases from  $-w/2$  to  $w/2$  (and still equals  $n\kappa$  at  $\xi=0$ ). Hence, the two ends of the spiral will never coincide and the resultant field will never have zero magnitude.

We have now proved that regardless of the physical open fraction, there are never missing orders in atom diffraction from a material structure unless  $C_3=0$ . This expands on the point already identified in [1] that phase shifts due to atom-surface interactions modify the envelope of the diffraction pattern.

The phasor diagram also provides a method to bound the error on numerically computed amplitudes. If the limits of integration in Eq. (2) are replaced by  $\pm(w/2 - \epsilon)$ , then the maximum error in the resultant amplitudes is given by the radius of a circle with the curvature of the phasor diagram at the endpoint, i.e., error in  $\Psi_n$  is less than  $\Psi_{inc}(R/d)$  where  $R^{-1} \equiv d\Phi_n/d\xi|_{\xi=(w/2-\epsilon)}$ .

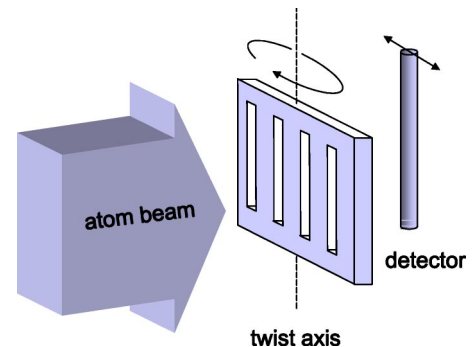


FIG. 3. Experimental geometry.

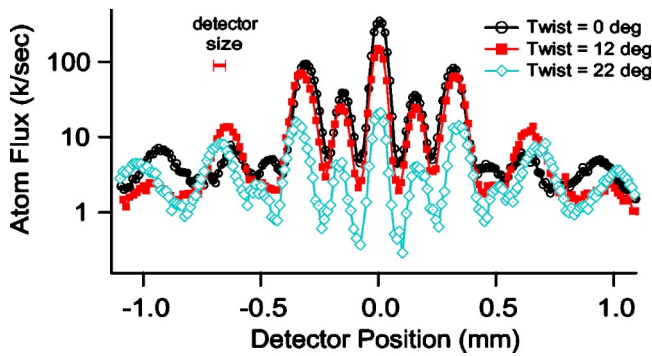


FIG. 4. (Color online) Diffraction scans with different grating twist. Diffraction of both sodium atoms and sodium dimers is visible. First order atom diffraction,  $I_1$ , is located at  $\pm 0.3$  mm from the 0th order.

To confirm this theoretical description, we present diffraction data using a beam composed of sodium atoms and sodium dimer molecules incident on a silicon nitride grating with a period of 100 nm. We call rotation about a grating bar *twist* as shown in Fig. 3. Normal incidence defines zero twist. Diffraction patterns shown in Fig. 4 were obtained by scanning the position of the hot-wire detector while the grating twist was fixed at 0, 12, and then 22°. Twist foreshortens the grating period and therefore slightly increases the diffraction angle. However, the  $+n$  and  $-n$  diffraction orders are nearly equally deflected because the atomic de Broglie wavelength is small compared to the grating spatial period.

The feature explored in this study is the relative intensity in each order, which changes considerably as the grating is twisted. Atom flux diffracted into the zeroth order decreases, but flux in the second and third orders oscillates as a function of grating twist. Figures 4 and 5 show that the second order intensity is maximized for an intermediate twist. Variation in the relative intensity among diffraction orders is expected because the projection of the grating viewed from the incident atom beam changes with twist. However, a model based on absorptive atom optics is not sufficient to explain our data. Phase shifts due to van der Waals interactions must be included, as discussed earlier.

We also present data obtained by scanning the grating twist while leaving the detector at one position (Fig. 5). In the latter experiment we have measured  $I_n = |\Psi_n|^2$  for each  $n = [0, 4]$  while continuously changing the projected open fraction. This technique is well suited to the task of searching for missing orders because the projected open fraction can be scanned through values that should cause missing orders according to the theory without atom-surface interactions (e.g.,  $\frac{1}{2}$ ,  $\frac{1}{3}$ , and  $\frac{1}{4}$ ).

For a perfectly thin grating, twist would not affect the open fraction. For our gratings, with a cross-section geometry shown in Fig. 6, twist does modify the projected open fraction. Furthermore, due to trapezoidal grating bars, van der Waals phase shifts must be carefully analyzed. With reference to Fig. 6, twisting the grating by angle  $\beta$  causes slots to appear narrower so the resulting open fraction is

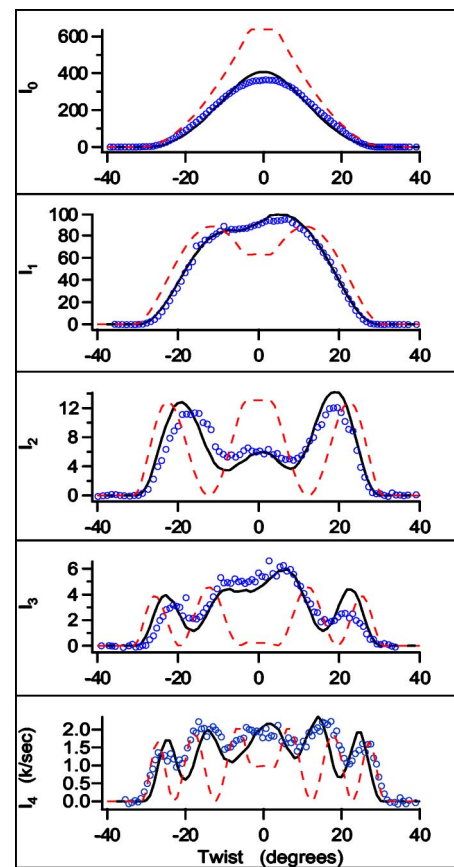


FIG. 5. (Color online) Data (circles) and models (dashed and solid lines) of the intensity in each diffraction order as a function of grating twist. The model parameters are:  $d=100$  nm,  $w=67$  nm,  $l=116$  nm, and  $\alpha=3.5^\circ$ . For dashed lines  $C_3=0$  [using Eq. (11)], and for solid lines  $C_3=5$  eV  $\text{\AA}^3$  [using Eq. (13)]. Statistical error bars for each data point are smaller than the circles.

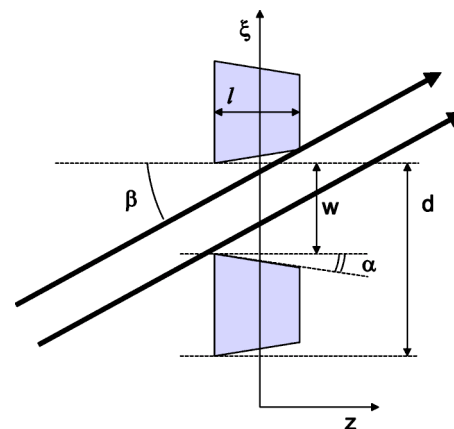


FIG. 6. Top view of the atom beam passing through the grating slots. The grating twist is denoted by  $\beta$ , the wedge angle of each bar is  $\alpha$ , the grating period is  $d$ , the thickness is  $l$ , and physical open width is  $w$ .

$$\eta(\beta) = \begin{cases} \frac{w}{d}, & |\beta| < \alpha, \\ \frac{w - l(\tan \beta - \tan \alpha)}{d}, & \alpha < |\beta| < \beta_{max}, \\ 0, & \beta_{max} < |\beta|, \end{cases} \quad (10)$$

where  $w$  is the slot width viewed at normal incidence,  $l$  is the thickness of the grating,  $\alpha$  is the wedge angle of the bars,  $\beta$  is the twist,  $\beta_{max}$  is the maximum twist at which any flux is transmitted, and  $d$  is the grating period viewed at normal incidence. The intensity in different diffraction orders then depends on twist as

$$I_n(\beta) = \eta(\beta)^2 \text{sinc}^2(\eta(\beta)n). \quad (11)$$

This model without an allowance for atom-surface interactions was used to predict intensity in the first five orders as a function of twist shown in Fig. 5 (dashed lines), and compares poorly with the data.

Two features of this model are familiar from standard diffraction theory. First, in the limit of small open fraction the intensity of each order becomes equal. This happens at large twist. Second, at certain angles for which  $\eta(\beta) = m/n$ , missing orders are predicted [as per Eq. (1)]. However, the observed atom beam flux is never entirely suppressed until the projected open fraction is zero. This demonstrates that there are no missing orders in the data.

Several of the grating geometry parameters are known from the manufacturing process and SEM images [7]. The period is  $d = 100$  nm and the window size is  $w = 67 \pm 5$  nm, so at normal incidence the open fraction is approximately 67%. The thickness,  $l$ , and wedge angle,  $\alpha$ , are constrained by measuring the maximum twist at which atoms are transmitted. These must satisfy the condition  $w = l(\tan \beta_{max} - \tan \alpha)$ , with the measured  $\beta_{max} = 31 \pm 2^\circ$ . With this constraint,  $\alpha$  is the only free parameter in the model before atom-surface interactions are included.

The relative intensity for each order is determined without interactions by Eq. (11), and can be compared to the data that were recorded without changing the detector gain or incident beam flux. However, the velocity distribution of the beam broadens the higher order diffraction peaks. Each diffraction order has a HWHM in the detector plane given approximately by  $\sigma_n^2 = \sigma_0^2 + [\Theta_n L(\sigma_v/v)]^2$  where  $\sigma_0$  is the HWHM of the zeroth order,  $L$  is the distance between the grating and the detector,  $\sigma_v/v$  is the ratio of the HWHM spread in velocity to the average velocity, and  $\Theta_n$  is the diffraction angle [2]. The velocity ratio is 1/15 and the average velocity is 1000 m/s. To allow for the velocity distribution, the relative intensity of each diffraction order is multiplied by  $\sigma_n^{-1}$  in the model. We have not accounted for the change in  $\Theta_n$  with twist, but we note this has the effect of further reducing the recorded intensity of the higher orders at large twist.

To include the van der Waals interactions with the twisted grating, the model must account for the varying distance to the surface as atoms pass through the slots as shown in Fig. 6, i.e., the transverse coordinate in the grating now depends on the longitudinal position  $\xi \rightarrow \xi_0 + z \tan \beta$ . The potential due to each interior wall is approximated by the van der

Waals potential for an infinite surface when the atoms are inside the grating slots, and zero elsewhere. Then the phase shift due to one wall of a twisted grating is

$$\phi_{vdW}(\xi_0) = \frac{C_3 [2\hbar v (\tan \alpha + \tan \beta) \cos \beta \cos^3 \alpha]^{-1}}{\left[ \frac{w}{2} + \left( \frac{l}{2} + z \right) \tan \alpha + \xi_0 + z \tan \beta \right]^2} \Bigg|_{z=-l/2}^{z=l/2} \quad (12)$$

and the phase shift due to the opposite wall is given by the same expression with the sign of  $\beta$  and  $\xi_0$  reversed. As before, the field amplitude in  $n$ th order diffraction is given by an integral, but now the limits of integration depend on grating twist, wedge angle, and thickness and so does  $\phi_{vdW}$  [as given by Eq. (12)]:

$$\Psi_n = \int_{\xi_{max}}^{\xi_{min}} e^{i[\phi_n(\xi_0) + \phi_{vdW}(\xi_0)]} d\xi_0. \quad (13)$$

The lower limit of integration is

$$\xi_{min} = \frac{-w}{2} + \frac{l}{2} \tan \beta, \quad (14)$$

and the upper limit of integration is

$$\xi_{max} = \begin{cases} \frac{w}{2} + \frac{l}{2} \tan \beta, & |\beta| < \alpha, \\ \frac{w}{2} + l \tan \alpha - \frac{l}{2} \tan \beta, & |\beta| > \alpha. \end{cases} \quad (15)$$

Equation (13) can now be used to describe intensity in each order as a function of van der Waals coefficient, atom velocity, and grating twist:  $I_n(C_3, v, \beta) = |\Psi_n|^2$ . When  $C_3$  is zero, the expression for the intensities reduces to Eq. (11). In comparison, when  $C_3$  is not zero the model predicts no missing orders and agrees qualitatively with the data in Fig. 5 (this model is shown with solid lines). We note the van der Waals interaction diverts flux from the zeroth order into the higher orders, and tends to smooth the features given by Eq. (11). Even the slight asymmetry in intensity as a function of twist is reproduced. To our knowledge this is the first hint of a material structure acting as a blazed grating for atom waves.

The maximum asymmetry we observe in the first order occurs at a twist of  $\pm 5^\circ$  and is  $I_1^{+5^\circ} / I_1^{-5^\circ} = 1.1$ . In simulations with a larger wedge angle and larger  $C_3$ , the asymmetry can be as large as 1.5. An asymmetric distribution of intensity between the +1 and -1 orders, as this implies, would be useful for atom interferometers that only employ the 0 and +1 diffraction orders.

When used to measure  $C_3$  for sodium atoms and a grating surface of silicon nitride, this experiment determines  $C_3 = 5_{-2}^{+5}$  eV  $\text{\AA}^3$  (statistical error only). This measurement is consistent with the theoretical value of  $C_3 = 7.6$  eV  $\text{\AA}^3$  for Na and a perfectly conducting wall [8], and also with the theoretical value of  $C_3 = 3.2$  eV  $\text{\AA}^3$  for a 1-oscillator Na atom and a surface made of silicon nitride calculated using the method outlined in [3]. Hence, no additional atom-surface interactions such as those due to ad-atoms reported in [10] are required to explain our data.

Uncertainty in the measured  $C_3$  could be reduced if the grating wedge angle,  $\alpha$ , and the grating window size  $w$  were more accurately known. Then  $\alpha$  would not be a free parameter, and any systematic uncertainty due to imperfect knowledge of  $w$  would be reduced. To motivate work with improved precision, we note that a gold coating on the surface of the grating bars should modify  $C_3$ . Measurements of this change would test the theoretical work of Zhou and Spruch [9]. Additionally, a search could be made for the effect of polarized ad-atoms by applying external electric fields on the grating [10].

In principle the experimental method presented here can also be used to verify the functional form of the atom-surface potential. However, the statistical agreement between the data presented here and various models using  $V(r)=-C_j/r^j$  does not allow us to discriminate between  $j=2, 3$  or  $4$ . To improve this study, three sources of uncertainty must be addressed. The detector should be relocated to the peak of each order as a function of grating twist. The grating geometric parameters ( $w$ ,  $l$ , and  $\alpha$ ) should each be independently measured. Finally, a theoretical model for the potential in all locations around the physical grating bars should be included in this analysis.

The absolute transmission efficiency of the grating is another concern. Even at normal incidence the van der Waals interaction has reduced the intensity of the zeroth-order diffraction by a factor of 0.65 compared to the zeroth-order flux

predicted with  $C_3=0$ . As an extrapolation, if we could obtain similar gratings with a 20 nm period, the flux transmitted into the zeroth order will be reduced to 0.06 of the flux predicted with  $C_3=0$ . Alternatively, if atoms slower than 1000 m/s were used, the transmission into zeroth-order diffraction will be further reduced. For example, 100 m/s atoms would have the intensity of the zeroth-order diffraction reduced by a factor of 0.28 compared to the zeroth-order flux predicted with  $C_3=0$ . This factor for atoms with a speed of 10 m/s would be 0.05. Hence, van der Waals interactions will have a large effect on sub-100-nanometer scale atom optics, or material atom optics with cold atoms.

In conclusion, a novel way to measure the atom-surface interaction potential was presented. By twisting a 100-nm period diffraction grating we show that atom-surface interactions prevent missing orders and cause asymmetric diffraction patterns. Both observations are explained by a complex transmission function and a phasor analysis similar to the Cornu spiral.

This work was supported by the Research Corporation. We thank T. Savas and H.I. Smith for fabricating the 100 nanometer period material gratings [7]. We also thank B. Anderson for a critical reading of this manuscript and both H. Uys and P. Hoerner for technical assistance.

- 
- [1] R. E. Grisenti, W. Schollkopf, J. P. Toennies, G. C. Hergerfeldt, and T. Kohler, *Phys. Rev. Lett.* **83**, 1755 (1999).
- [2] R. E. Grisenti, W. Schollkopf, J. P. Toennies, J. R. Manson, T. A. Savas, and H. I. Smith, *Phys. Rev. A* **61**, 033608 (2000).
- [3] R. Bruhl, P. Fouquet, R. E. Grisenti, J. P. Toennies, G. C. Hergerfeldt, T. Kohler, M. Stoll, and D. Walter, *Europhys. Lett.* **59**, 357 (2002).
- [4] E. Hecht, *Optics* (Addison-Wesley, Redwood City, CA, 1990).
- [5] D. Halliday, R. Resnick, and K. Krane, *Physics* (Wiley, New York, 2002).
- [6] P. W. Milonni, *The Quantum Vacuum* (Academic, New York, 1994).
- [7] T. A. Savas, M. L. Schattenburg, J. M. Carter, and H. I. Smith, *J. Vac. Sci. Technol. B* **14**, 4167 (1996).
- [8] A. Derevianko, W. Johnson, M. Safranov, and J. Baab, *Phys. Rev. Lett.* **82**, 3589 (1999).
- [9] F. Zhou and L. Spruch, *Phys. Rev. A* **52**, 297 (2004).
- [10] J. M. McGuirk, D. M. Harber, J. M. Obrecht, and E. A. Cornell, *Phys. Rev. A* **69**, 062905 (2004).